Asian Journal of Chemistry; Vol. 38, No. 11 (2026), 3061-3068
ASIAN JOURNAL OF CHEMISTRY
https://doi.org/10.14233/ajchem.2026.36628

Synthesis, Characterization and Anti-inflammatory Evaluation of Novel 1,2,4-Triazole-Based Hept-6-ene-1,3,5-trione Analogues

SONIYA SATPUTE[1], POONAM JADHAV[2], VANITA KATORE[3], ARSHU PATEL[4], DATTATRAYA THORAT[5] and AJAY MULE[4,*]

[1]Department of Pharmaceutical Chemistry, Pravara Rural Education Society's College of Pharmacy (D & B Pharm), Chincholi-422102, India
[2]Department of Pharmaceutical Chemistry, Dr. Naikwadi College of Pharmacy, Jamgao, Sinner-422113, India
[3]Department of Pharmaceutical Chemistry, Samarth College of Pharmacy, Belhe-412410, India
[4]Department of Pharmacognosy, Pravara Rural College of Pharmacy, Loni-413736, India
[5]Department of Pharmaceutical Chemistry, Pravara Institute of Medical Sciences (Deemed to be University), College of Pharmaceutical Sciences, Loni-413736, India

*Corresponding author: E-mail: mulfajay30@gmail.com

Received: 25 July 2026 *Accepted*: 17 October 2026 *Published online*: 13 November 2026 AJC-22537

In this study, a series of eight 1,2,4-triazole-based hept-6-ene-1,3,5-trione analogues (**AM-1-8**) was designed and synthesized by combining a triazole-bearing aromatic group with a curcuminoid-inspired triketone framework. The compounds were obtained through a key triketone intermediate followed by Claisen-Schmidt condensation with appropriately substituted aromatic aldehydes, yielding the final products in the range of 49-81%. Structural characterization was performed using infrared spectroscopy, nuclear magnetic resonance and mass spectrometry. Molecular docking against COX-2 (PDB: 3NT1) and computational ADMET and toxicity profiling using SwissADME and ProTox-II were undertaken as preliminary assessments of their pharmacological properties. Compound **AM-6** bearing an *o*-hydroxyphenyl substituent, received the most favourable docking score (-8.7 kcal/mol). The anti-inflammatory activity of the synthesized analogues was investigated *in vivo* using the carrageenan-induced paw edema model in Wistar rats, with diclofenac sodium as the reference drug. All eight analogues exhibited lower paw volumes than the disease control at the later observation time points. Compound **AM-6** recorded the lowest paw volume (4.05) at 150 min, compared with 4.80 for diclofenac sodium. ProTox-II predictions revealed potential toxicity-related liabilities, precluding any preliminary claim of safety.

Keywords: 1,2,4-Triazoles, Cyclooxygenase-2, Molecular docking, Carrageenan-induced paw edema, ADMET.

INTRODUCTION

Heterocyclic compounds are important scaffolds in the medicinal chemistry due to their structural diversity and ability to modulate the molecular interactions and physicochemical properties, making them valuable for developing biologically active molecules [1,2]. Among nitrogen-containing heterocycles, the 1,2,4-triazole ring has attracted considerable interest due to its chemical stability, electron-rich nitrogen atoms and potential to participate in hydrogen-bonding and other non-covalent interactions. Substitution at different positions of this ring provides opportunities to modify biological activity and molecular properties. Several 1,2,4-triazole derivatives have been investigated for diverse pharmacological applications, supporting the continued exploration of this scaffold in medicinal chemistry [3-6].

The biological properties of heterocyclic compounds are strongly influenced by the nature and arrangement of their attached functional groups. Conjugated carbonyl systems, particularly enone and β-dicarbonyl units, offer additional structural features that can influence molecular conformation, electronic distribution and intermolecular interactions. In this context, curcumin and related conjugated carbonyl compounds have received attention in inflammation related research, providing a chemical basis for exploring modified carbonyl containing frameworks [7]. The combination of a heterocyclic unit with a conjugated carbonyl framework may therefore provide a useful approach for generating structurally distinct molecules with potentially relevant biological properties. Such molecular hybridization allows the electronic and steric characteristics of individual structural units to be examined within a common molecular framework.

This is an open access journal, and articles are distributed under the terms of the Attribution 4.0 International (CC BY 4.0) License. This license lets others distribute, remix, tweak, and build upon your work, even commercially, as long as they credit the author for the original creation. You must give appropriate credit, provide a link to the license, and indicate if changes were made.

Inflammation is a complex biological response involving cellular and molecular mediators that regulate tissue injury and repair. Persistent or dysregulated inflammatory processes are implicated in several pathological conditions, making the development of anti-inflammatory agents an important area of pharmaceutical research [8]. Non-steroidal anti-inflammatory drugs (NSAIDs) exert their principal pharmacological effects through inhibition of cyclooxygenase (COX), the enzyme responsible for prostaglandin biosynthesis [9]. COX-1 and COX-2 differ in their expression patterns and physiological roles, and inhibition of these isoforms contributes to both the therapeutic effects and adverse reactions of NSAIDs. Prolonged use of conventional NSAIDs is associated with gastrointestinal, renal and cardiovascular complications, underscoring the need to investigate alternative chemical structures with potential anti-inflammatory activity [10,11].

Molecular docking provides a computational approach for examining the possible binding orientation and interactions of small molecules within a protein binding site. The COX-2 structure complexed with naproxen (PDB ID: 3NT1) was selected for the docking assessment in this study [12,13]. SwissADME was used to estimate selected physico-chemical and pharmacokinetic properties [14], while ProTox-II was employed for preliminary toxicity prediction [15].

The present study describes the synthesis of eight unsymmetrical, open-chain 1,2,4-triazole-containing hept-6-ene-1,3,5-trione analogues (**AM-1-8**). The molecular framework comprises a 4-(1*H*-1,2,4-triazol-1-yl)phenyl group linked to a substituted aryl-conjugated enone through a tricarbonyl chain, differing from the symmetrical diaryl structure of curcumin. The terminal aromatic ring was varied with electron-donating (methoxy and dimethylamino), electron withdrawing (chloro and nitro) and hydroxy substituents to examine their influence on biological activity. Molecular docking, *in silico* ADMET and toxicity predictions were performed to assess their pharmacological profiles. Anti-inflammatory activity was evaluated using the carrageenan-induced paw oedema model in Wistar rats, with diclofenac as the reference drug [16]. The study examines the influence of structural variations on the biological response of the synthesized analogues.

EXPERIMENTAL

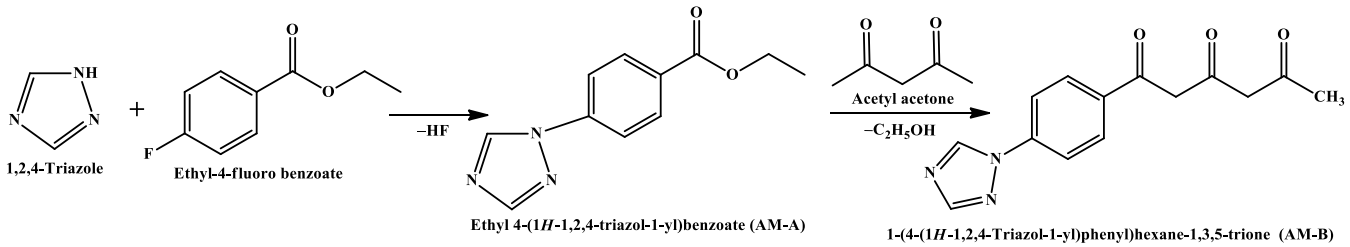
The chemicals and solvents, ethyl 4-hydroxybenzoate, 1,2,4-triazole, potassium carbonate, acetylacetone, DMSO, ethanol, DMF, sodium ethoxide, sodium hydroxide, glacial acetic acid, ethyl acetate, *n*-hexane and brine (all procured from Merck Ltd., India) were used for the synthesis and purification of the target compounds. Carrageenan and diclofenac sodium used in the pharmacological studies were of laboratory grade.

The synthesized compounds were characterized by IR, ^{1}H NMR and ESI-MS. Melting points were determined using open capillary tubes without correction. IR spectra were recorded using a Fourier-transform infrared (FTIR) spectrometer (Shimadzu IRSpirit) with KBr pellets. ^{1}H NMR spectra were acquired using a 500 MHz NMR spectrometer (Bruker Avance III HD 500 MHz), with $CDCl_3$/DMSO-d_6 as the solvent and TMS as the internal standard. Mass spectra were recorded using an electrospray ionization mass spectrometer (Agilent 6120 LC/MS). TLC was performed on silica gel 60 F_{254} plates and visualized under UV light.

Synthesis of ethyl 4-(1*H*-1,2,4-triazol-1-yl)benzoate (intermediate AM-A): Ethyl 4-(1*H*-1,2,4-triazol-1-yl)benzoate was synthesized by nucleophilic aromatic substitution of ethyl 4-fluorobenzoate with 1,2,4-triazole. Ethyl 4-fluorobenzoate (2.0 g) and potassium carbonate (1.5 g) were added to a dry 50 mL round-bottom flask containing dry DMSO (10 mL). 1,2,4-Triazole (1.2 g) was added and the reaction mixture was stirred at room temperature for 15-30 min. The mixture was then heated at 90-100 ºC for 6-8 h under a nitrogen or argon atmosphere with continuous stirring. Reaction progress was monitored by TLC. After completion, the mixture was cooled to room temperature and poured into cold distilled water (50 mL). The aqueous mixture was extracted with ethyl acetate (3 × 20 mL). The combined organic layers were washed with brine, dried over anhydrous sodium sulphate, filtered and concentrated under reduced pressure. The crude product was purified by silica gel column chromatography using ethyl acetate and *n*-hexane (30:70, v/v) to obtain intermediate **AM-A**. Yield: 78.34%; R_f: 0.68 (silica gel, ethyl acetate: hexane); m.p.: 186-188 ºC. IR (KBr, ν_{max}, cm^{-1}): 3090 (Ar–H), 2983 (C–H), 1702 (C=O, ester), 1602 (C=N, triazole), 1514 (Ar C=C), 1359 (C–N), 1275 (C–O), 1100 (C–O–C), 818, 772, 697 (Ar–H), 649 (Ar *def.*). ^{1}H NMR (500 MHz, $CDCl_3$, δ ppm): 9.09 (d, *J* = 1.6 Hz, 1H), 8.16 (d, *J* = 1.6 Hz, 1H), 7.99-7.93 (m, 2H), 7.64-7.58 (m, 2H), 4.39 (q, *J* = 7.1 Hz, 2H), 1.40 (t, *J* = 7.1 Hz, 3H); MS (ESI): *m/z* $[M+H]^+$ calcd. 218.09 for $C_{11}H_{11}N_3O_2$; 218.15.

Synthesis of 1-(4-(1*H*-1,2,4-triazol-1-yl)phenyl)hexane-1,3,5-trione (intermediate AM-B): The key triketone intermediate AM-B was synthesized by Claisen-type acylation of acetylacetone with ethyl 4-(1*H*-1,2,4-triazol-1-yl)benzoate. The aromatic ester (200 mg) was dissolved in dry ethanol (5 mL) followed by the addition of sodium ethoxide (100 mg). The mixture was stirred at room temperature for 10 min, and acetylacetone (150 mg) was added dropwise. The reaction mixture was heated under reflux at 70-80 ºC for 6-8 h under a nitrogen atmosphere. Reaction progress was monitored by TLC (**Scheme-I**). After completion, the mixture was cooled to room temperature and acidified with dilute HCl. The product was extracted with ethyl acetate (3 × 20 mL), and the combined organic layers were washed with brine, dried over anhydrous sodium sulphate, filtered and concentrated under reduced pressure. The crude product was purified by silica gel column chromatography using an appropriate ethyl acetate/*n*-hexane solvent system to obtain **AM-B**. Yield: 68.34%; R_f: 0.58 (silica gel, ethyl acetate:*n*-hexane); m.p.: 182-188 ºC; IR (KBr, ν_{max}, cm^{-1}): 3454 (O–H, enol form), 3034 (Ar–H), 1746 (C=O), 1640 (C=N), 1540, 1491 (arom. C=C), 1396, 1341 (C–N), 1244, 1191, 1142 (C–O), 795, 714 (arom. C–H bend.), 676 (arom. ring def.); ^{1}H NMR (500 MHz, $CDCl_3$, δ ppm): 9.09 (d, *J* = 1.6 Hz, 1H), 8.16 (d, *J* = 1.6 Hz, 1H), 8.02-7.96 (m, 2H), 7.64-7.58 (m, 2H), 4.07 (s, 2H), 3.65 (s, 2H); ESI-MS: $C_{14}H_{14}N_3O_3^+$ $[M + H]^+$: 272.1030; found: *m/z* 271.09.

General procedure for synthesis of triazole analogues (AM 1-8): The target analogues were synthesized by Claisen-Schmidt condensation of intermediate **AM-B** with substi-



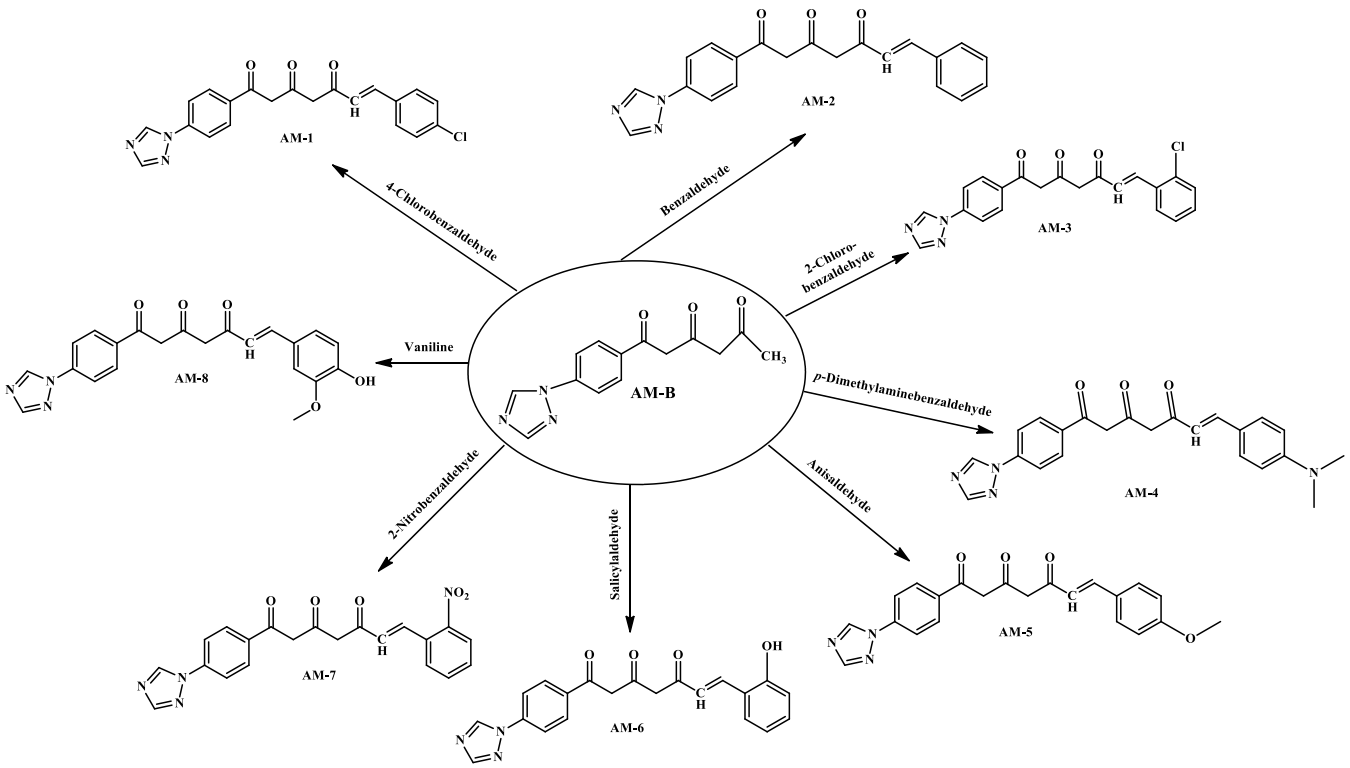
Scheme-I: Synthetic pathway of triazole–triketone analogues

tuted aromatic aldehydes. **AM-B** (271 mg, 1 mmol) was dissolved in absolute ethanol (10 mL) in a 50 mL round-bottom flask. The appropriate aromatic aldehyde (1 mmol) was added followed by dropwise addition of 10% (w/v) aqueous NaOH (1 mL). The reaction mixture was stirred at 40-50 ºC for 4-6 h and reaction progress was monitored by TLC using ethyl acetate/*n*-hexane (1:1, v/v) (**Scheme-II**). After completion, the mixture was cooled to room temperature, neutralized to pH 6-7 with glacial acetic acid and poured into ice-cold water (50 mL). The precipitated solid was collected by filtration, washed with cold water (3 × 10 mL) and dried under vacuum. Recrystallization from ethanol or ethanol/DMF afforded the target compounds in 49-81% yield.

(*E*)-1-(4-(1*H*-1,2,4-triazol-1-yl)phenyl)-7-(4-chlorophenyl)hept-6-ene-1,3,5-trione (AM-1): Yield: 67%; R_f (silica gel, ethyl acetate:*n*-hexane): 0.78; m.p.: 125-127 ºC; IR (KBr, ν_{max}, cm^{-1}): 3139 (Ar–H/triazole C–H), 3046 (=C–H), 1716, 1677 (C=O), 1611 (triazole ring *str*.), 1554–1493 (arom. C=C), 1276 (C–N), 858 (C–H out-of-plane *bend*.), 751, 663 (arom. ring *def*./C–Cl); ^{1}H NMR (500 MHz, DMSO-d_6, δ ppm): 9.10 (s, 1H, triazole-H), 8.17 (s, 1H, triazole-H), 8.05-7.95 (m, 2H, triazole-substituted phenyl-H), 7.65-7.55 (m, 2H, triazole-substituted phenyl-H), 7.45-7.30 (m, 4H, chlorophenyl-H), 7.15-6.95 (m, 2H, olefinic-H), 4.10-3.85 (m, 4H, methylene-H); MS (ESI): *m/z* $[M+H]^+$ calcd. 394.10 for $C_{21}H_{16}ClN_3O_3$; found: *m/z*: 394.53.

(*E*)-1-(4-(1*H*-1,2,4-triazol-1-yl)phenyl)-7-phenyl) hept-6-ene-1,3,5-trione (AM-2): Yield: 51%; R_f: 0.69 (silica gel, ethyl acetate:*n*-hexane); m.p.: 124-126 ºC. IR (KBr, ν_{max}, cm^{-1}): 3102 (arom./triazole C–H), 3008 (=C–H), 1717, 1654 (C=O, trione), 1541 (C=N, triazole), 1493 (arom. C=C), 1262 (C–N, triazole), 1160 (C–N *str*.), 984 (*trans* CH=CH), 842, 792 (substituted arom. ring); ^{1}H NMR (500 MHz, DMSO-d_6, δ ppm): 9.12 (s, 1H, triazole-H), 8.17 (s, 1H, triazole-H), 8.05-7.95 (m, 2H, triazole-substituted phenyl-H), 7.65-7.55 (m, 2H, triazole-substituted phenyl-H), 7.45-7.20 (m, 5H, phenyl-H), 7.15-6.95 (m, 2H, olefinic-H), 4.10-3.85 (m, 4H, methylene-H); MS (ESI): *m/z* $[M+H]^+$ calcd. 360.13 for $C_{21}H_{17}N_3O_3$; found: *m/z*: 360.17.

(*E*)-1-(4-(1*H*-1,2,4-triazol-1-yl)phenyl)-7-(2-chlorophenyl)hept-6-ene-1,3,5-trione (AM-3): Yield: 49%; R_f: 0.70 (silica gel, ethyl acetate:*n*-hexane); m.p.: 140-142 ºC; IR



Scheme-II: Chemical structures of synthesized analogues **AM-1–AM-8**

(KBr, ν_{max}, cm^{-1}): 3016 (arom. C–H *str*.), 2953, 2872 (aliph. C–H *str*.), 1702, 1646 (C=O *str*.), 1634 (triazole ring *str*.), 1567-1490 (arom. C=C *str*.), 1263 (C–N *str*.), 1194 (fingerprint-region vibration), 916 (C–H out-of-plane *bend*.), 873, 747 (arom. C–H *bend*.), 644 (C–Cl); ^{1}H NMR (500 MHz, DMSO-d_6, δ ppm): 9.15 (s, 1H, triazole-H), 8.21 (s, 1H, triazole-H), 8.06 (d, *J* = 8.5 Hz, 2H, Ar-H), 7.66 (d, *J* = 8.5 Hz, 2H, Ar-H), 7.52 (dd, J = 7.8, 1.5 Hz, 1H, chlorophenyl-H), 7.38-7.28 (m, 2H, chlorophenyl-H), 7.18 (dd, *J* = 7.8, 1.5 Hz, 1H, chlorophenyl-H), 7.27 (d, *J* = 15.5 Hz, 1H, CH=CH), 7.04 (d, *J* = 15.5 Hz, 1H, CH=CH), 4.11 (s, 2H, CH_2), 3.94 (s, 2H, CH_2); MS (ESI): *m/z* $[M+H]^+$ calcd. 394.10 for $C_{21}H_{16}ClN_3O_3$; found: *m/z*: 394.17.

(*E*)-1-(4-(1*H*-1,2,4-triazol-1-yl)phenyl)-7-(4-(dimethylamino)phenyl)hept-6-ene-1,3,5-trione (AM-4): Yield: 59%; R_f: 0.50 (silica gel, ethyl acetate:*n*-hexane); m.p.: 110-112 ºC; IR (KBr, ν_{max}, cm^{-1}): 3121 (arom./triazole C–H *str*.), 2975, 2877 (aliph. C–H *str*.), 1695, 1646 (C=O *str*.), 1594 (triazole ring *str*.), 1505-1474 (arom. C=C *str*.), 1269 (C–N *str*.), 1159, 1108 (fingerprint-region vibrations), 1017 (arom. C–H *bend*.), 768, 679 (ring *def*./C–X); ^{1}H NMR (500 MHz, DMSO-d_6, δ ppm): 9.09 (d, *J* = 1.6 Hz, 1H), 8.16 (d, *J* = 1.6 Hz, 1H), 8.02-7.96 (m, 1H), 7.64-7.49 (m, 3H), 6.85-6.79 (m, 1H), 6.74 (dt, *J* = 16.1, 0.9 Hz, 1H), 4.07 (s, 1H), 3.55 (d, *J* = 0.9 Hz, 1H), 2.92 (s, 3H); MS (ESI): *m/z* $[M+H]^+$ calcd. 403.18 for $C_{23}H_{22}N_4O_3$; found: *m/z*: 403.26.

(*E*)-1-(4-(1*H*-1,2,4-triazol-1-yl)phenyl)-7-(4-methoxyphenyl)hept-6-ene-1,3,5-trione (AM-5): Yield: 74%; R_f: 0.65 (silica gel, ethyl acetate:*n*-hexane); m.p.: 117-119 ºC; IR (KBr, ν_{max}, cm^{-1}): 3043 (arom./=C–H *str*.), 2998, 2918 (aliph. C–H *str*.), 1669 (C=O *str*.), 1637 (triazole ring *str*.), 1597-1490 (arom. C=C *str*.), 1289-1238 (C–O/C–N *str*.), 1175, 1140 (C–O *str*.), 1014 (arom. C–H *bend*.), 709, 633 (ring *def*.); ^{1}H NMR (500 MHz, DMSO-d_6, δ ppm): 9.10 (s, 1H, triazole-H), 8.17 (s, 1H, triazole-H), 8.00 (d, *J* = 8.5 Hz, 2H, Ar-H), 7.61 (d, *J* = 8.5 Hz, 2H, Ar-H), 7.31 (d, *J* = 8.7 Hz, 2H, methoxyphenyl-H), 6.88 (d, *J* = 8.7 Hz, 2H, methoxyphenyl-H), 7.13 (d, *J* = 15.7 Hz, 1H, CH=CH), 6.94 (d, *J* = 15.7 Hz, 1H, CH=CH), 4.06 (s, 2H, CH_2), 3.89 (s, 2H, CH_2), 3.82 (s, 3H, OCH_3); MS (ESI): *m/z* $[M+H]^+$ calcd. 390.14 for $C_{22}H_{19}N_3O_4$; found: *m/z* 390.64.

(*E*)-1-(4-(1*H*-1,2,4-triazol-1-yl)phenyl)-7-(2-hydroxyphenyl)hept-6-ene-1,3,5-trione (AM-6): Yield: 80.64%; R_f: 0.81 (silica gel, ethyl acetate:*n*-hexane); m.p.: 92-94 ºC; IR (KBr, ν_{max}, cm^{-1}): 3208 (arom./triazole C–H), 3042 (=C–H), 2961, 2843 (aliph. C–H), 1663 (C=O, trione), 1570 (C=N, triazole), 1539-1489 (arom. C=C), 1389-1331 (C–N *str*.), 1202, 1139, 1076 (C–O/C–N *str*.), 926 (*trans* CH=CH), 711, 665 (Ar C–H out-of-plane *bend*.); ^{1}H NMR (500 MHz, DMSO-d_6, δ ppm): 9.13 (s, 1H, triazole-H), 8.20 (s, 1H, triazole-H), 8.04 (d, *J* = 8.5 Hz, 2H, Ar-H), 7.64 (d, *J* = 8.5 Hz, 2H, Ar-H), 7.42 (dd, J = 7.8, 1.5 Hz, 1H, hydroxyphenyl-H), 7.20 (td, *J* = 7.8, 1.5 Hz, 1H, hydroxyphenyl-H), 6.91 (d, *J* = 8.2 Hz, 1H, hydroxyphenyl-H), 6.83 (td, *J* = 7.8, 1.0 Hz, 1H, hydroxyphenyl-H), 7.24 (d, *J* = 15.6 Hz, 1H, CH=CH), 7.02 (d, *J* = 15.6 Hz, 1H, CH=CH), 4.09 (s, 2H, CH_2), 3.92 (s, 2H, CH_2), 10.0-12.0 (br s, 1H, phenolic OH); MS (ESI): *m/z* $[M+H]^+$ calcd. 376.13 for $C_{21}H_{17}N_3O_4$; found: *m/z* 376.26.

(*E*)-1-(4-(1*H*-1,2,4-triazol-1-yl)phenyl)-7-(2-nitrophenyl)hept-6-ene-1,3,5-trione (AM-7): Yield: 78.23%; R_f: 0.74 (silica gel, ethyl acetate:*n*-hexane); m.p.: 118-120 ºC; ^{1}H NMR (500 MHz, DMSO-d_6, δ ppm): 9.18 (s, 1H, triazole-H), 8.25 (s, 1H, triazole-H), 8.10 (d, *J* = 8.5 Hz, 2H, Ar-H), 7.70 (d, *J* = 8.5 Hz, 2H, Ar-H), 7.82 (dd, J = 8.0, 1.5 Hz, 1H, nitrophenyl-H), 7.62 (td, J = 7.8, 1.5 Hz, 1H, nitrophenyl-H), 7.53 (td, *J* = 7.8, 1.2 Hz, 1H, nitrophenyl-H), 7.38 (dd, *J* = 7.8, 1.2 Hz, 1H, nitrophenyl-H), 7.35 (d, *J* = 15.4 Hz, 1H, CH=CH), 7.12 (d, *J* = 15.4 Hz, 1H, CH=CH), 4.14 (s, 2H, CH_2), 3.97 (s, 2H, CH_2). MS (ESI): *m/z* $[M+H]^+$ calcd. 405.12 for $C_{21}H_{16}N_4O_5$; found: *m/z* 405.12.

(*E*)-1-(4-(1*H*-1,2,4-triazol-1-yl)phenyl)-7-(4-hydroxy-3-methoxyphenyl)hept-6-ene-1,3,5-trione (AM-8): Yield: 72.56%; R_f: 0.65 (silica gel, ethyl acetate:*n*-hexane); m.p.: 140-142 ºC; IR (KBr, ν_{max}, cm^{-1}): 3050 (arom. C–H), 2990, 2860 (aliph. C–H), 1728, 1669 (C=O, trione), 1636 (C=N, triazole), 1570-1500 (arom. C=C), 1396-1313 (C–N *str*.), 1211, 1101 (C–O/C–N *str*.), 767, 718, 667 (arom. C–H out-of-plane *bend*.); ^{1}H NMR (500 MHz, DMSO-d_6, δ ppm): 9.11 (s, 1H, triazole-H), 8.18 (s, 1H, triazole-H), 8.01 (d, *J* = 8.5 Hz, 2H, Ar-H), 7.62 (d, J = 8.5 Hz, 2H, Ar-H), 7.12 (d, *J* = 1.8 Hz, 1H, aromatic-H), 7.05 (dd, *J* = 8.2, 1.8 Hz, 1H, arom.-H), 6.84 (d, *J* = 8.2 Hz, 1H, arom.-H), 7.14 (d, *J* = 15.7 Hz, 1H, CH=CH), 6.95 (d, *J* = 15.7 Hz, 1H, CH=CH), 4.07 (s, 2H, CH_2), 3.90 (s, 2H, CH_2), 3.86 (s, 3H, OCH_3), 5.0-9.0 (br s, 1H, phenolic OH); MS (ESI): *m/z* $[M+H]^+$ calcd. 406.14 for $C_{22}H_{19}N_3O_5$; found: *m/z* 406.42.

Molecular docking: Molecular docking was performed as a hypothesis-generating approach to investigate the potential binding interactions of **AM-1** to **AM-8** with COX-2. The crystal structure of mouse COX-2 complexed with naproxen (PDB ID: 3NT1; resolution 1.73 Å) was obtained from the Protein Data Bank. The protein structure was prepared using BIOVIA Discovery Studio Visualizer 2021 by removing water molecules and the co-crystallized ligand. Polar hydrogens were added and partial charges were assigned using AutoDock Tools 1.5.7. The structures of **AM-1** to **AM-8** and the reference drugs naproxen and diclofenac were energy-minimized using the MMFF94 force field in Open Babel. Molecular docking was performed using PyRx 0.8 with AutoDock Vina, employing an exhaustiveness setting of 8 [17,18]. An initial grid box of 25 × 25 × 25 Å was selected to encompass the naproxen-binding region of the COX-2 active-site channel. The grid centre was defined using the coordinates of the co-crystallized naproxen binding site. Key residues considered during interaction analysis included Arg120, Tyr355, Tyr385, Ser530, Val523 and Arg513. The docking protocol was evaluated by re-docking naproxen into the prepared receptor, followed by comparison of the crystallographic and predicted binding poses using RMSD. The docking scores and intermolecular interactions including hydrogen bonds, π-π interactions and hydrophobic contacts, were analyzed using BIOVIA Discovery Studio Visualizer 2021.

***In silico* ADMET and toxicity prediction:** The drug-likeness and pharmacokinetic properties of AM **1-8** were evaluated using the SwissADME web platform. The assessment included calculated lipophilicity (log P), hydrogen-bond donor and acceptor counts, rotatable bonds, bioavailability score,

gastrointestinal (GI) absorption and compliance with Lipinski, Ghose, Veber, Egan and Muegge drug-likeness filters. Pan-assay interference compound (PAINS) alerts and synthetic accessibility scores were examined to identify potential assay related liabilities and assess the feasibility of further structural modification. SwissADME predictions were generated using the default settings [14,19-23].

Toxicological profiles were estimated using the ProTox-II platform under its default settings. The evaluated parameters included predicted median lethal dose (LD_{50}, mg/kg), toxicity class and probability scores for available toxicity endpoints, such as hepatotoxicity, carcinogenicity, mutagenicity and cytotoxicity. Predictions related to molecular targets and biological barriers including the blood-brain barrier (BBB), estrogen receptor (ER), p53 and cytochrome P450 isoforms CYP3A4 and CYP2E1, were considered where available. The predicted LD_{50} values for AM **1-8** were predominantly classified as toxicity class 4. The reported prediction accuracy of 54.26% was considered when interpreting the results, indicating the need for caution in assessing the reliability of these computational estimates. The predictions were used for preliminary qualitative comparison of the analogues and do not establish their safety or toxicological profiles. Experimental studies are required to validate the predicted pharmacokinetic and toxicity characteristics.

In vivo anti-inflammatory activity

Animals: The *in vivo* anti-inflammatory activity of the synthesized analogues was evaluated in Wistar albino rats of either sex (male and female), weighing approximately 240 g and aged 8-10 weeks, using the carrageenan-induced paw edema model. The experimental protocol was reviewed and approved by the Institutional Animal Ethics Committee (IAEC), Pravara Rural College of Pharmacy (PRCOP), Loni, in accordance with the guidelines of the Committee for Control and Supervision of Experiments on Animals (CCSEA), Government of India (Approval No. CCSEA/IAEC/PRCOP/2026/09A). The study was conducted in accordance with the ARRIVE guidelines. The animals were obtained from the institutional animal facility and acclimatized to laboratory conditions for seven days before the experiment. They were housed in clean metallic cages in a well-ventilated animal room and maintained on a standard laboratory pellet diet with free access to drinking water. Food was withheld overnight before the experiment, while water was provided *ad libitum*.

The animals were randomly divided into 11 groups, with six animals in each group (n = 6), giving a total of 66 animals. Group I served as the normal control and received the vehicle alone without carrageenan administration. Group II served as the disease control and received carrageenan without any anti-inflammatory treatment. Group III received diclofenac sodium (25 mg/kg, orally) and served as the standard treatment group. Groups IV-XI received AM-1, AM-2, AM-3, AM-4, AM-5, AM-6, AM-7 and AM-8, respectively, by oral administration at the doses specified in the experimental protocol. The test compounds were suspended in a suitable vehicle and administered at a fixed volume based on body weight. Diclofenac sodium was used as the reference non-steroidal anti-inflammatory drug (NSAID).

Carrageenan-induced paw edema assay: Acute inflammation was induced by subplantar injection of a 1% (w/v) carrageenan solution into the right hind paw of each rat following oral administration of the respective test compound or control treatment. Paw volume was measured using a digital plethysmometer at 0, 30, 60, 90, 120 and 150 min after carrageenan injection. The increase in paw volume relative to the baseline measurement (0 min) was calculated as an indicator of edema formation [16]. The percentage inhibition of edema was calculated for each treated group at each time point relative to the disease control group using the following equation:

$$\text{Inhibition (\%)} = \frac{\Delta V_c - \Delta V_t}{\Delta V_c} \times 100$$

where ΔV_c and ΔV_t are the mean increases in paw volume relative to the 0 min baseline in the disease control and treated groups, respectively. Carrageenan was injected in a volume of (0.1 mL) and paw volume was measured with a digital plethysmometer.

Statistical analysis: The results are expressed as mean ± SD (n = 6). Statistical analysis was performed using GraphPad Prism (version 10.0). Differences among the experimental groups at each time point were evaluated by one-way analysis of variance (ANOVA) followed by Dunnett's multiple comparison test to compare each treatment group with the disease control group. A p-value < 0.05 was considered statistically significant.

RESULTS AND DISCUSSION

The target series **AM 1-8** was synthesized through a stepwise synthetic sequence involving the formation of ethyl 4-(1*H*-1,2,4-triazol-1-yl)benzoate followed by synthesis of the key triketone intermediate, 1-(4-(1*H*-1,2,4-triazol-1-yl)-phenyl)hexane-1,3,5-trione. Subsequent Claisen-Schmidt condensations with different aromatic aldehydes afforded the corresponding analogues. Recrystallization from ethanol or ethanol/DMF mixtures yielded crystalline products in moderate to good isolated yields (49-81%). The infrared spectra exhibited characteristic absorption bands attributable to the triketone carbonyl groups, aromatic C=C stretching vibrations and the 1,2,4-triazole ring. These spectral features are consistent with the principal functional groups incorporated into the designed molecular framework.

Molecular docking: Molecular docking calculations were performed using the naproxen-bound COX-2 crystal structure (PDB ID: 3NT1). Compound **AM-6** exhibited the most favourable predicted score (-8.7 kcal/mol) followed by **AM-1** and **AM-3** (-7.9 kcal/mol each) and AM-2 (-7.8 kcal/mol). (Table-1). These values represent computational estimates of ligand–receptor interactions and cannot be considered experimental binding affinities or direct evidence of COX-2 inhibition. The principal residues associated with the catalytic channel which include Arg120, Tyr355, Tyr385, Ser530 and Glu524, together with residues lining the side pocket (Fig. 1) [12].

***In silico* drug-likeness and toxicity:** SwissADME analysis was performed to evaluate the preliminary drug-likeness

TABLE-1
COX-2 DOCKING SCORES AND PRINCIPAL BINDING INTERACTIONS OF **AM-1–AM-8**

Compound	Docking score (kcal/mol)	No. of H-bond interactions	Main interacting residues*
AM-1	-7.9	2	ASN375, GLY225, TRP139, PHE142, LEU145
AM-2	-7.8	4	ASN34, GLN327, VAL155, ALA156, MET48
AM-3	-7.9	3	TYR122, SER126, SER121
AM-4	-7.1	3	GLN327, GLY135, CYS47, TYR136, PRO35, ALA156
AM-5	-6.4	4	LYS251, ASN310, ARG307, VAL261
AM-6	-8.7	4	LEU366, THR60, ASP125, GLN369, ARG44, PRO542
AM-7	-7.6	7	LEU238, ARG333, TRP139, ASN144, SER143, LEU224
AM-8	-7.7	6	LEU145, GLY235, ASN144, ASP229, GLU236, GLU140

*Preliminary values from the original docking run; replace with the validated re-docking results.

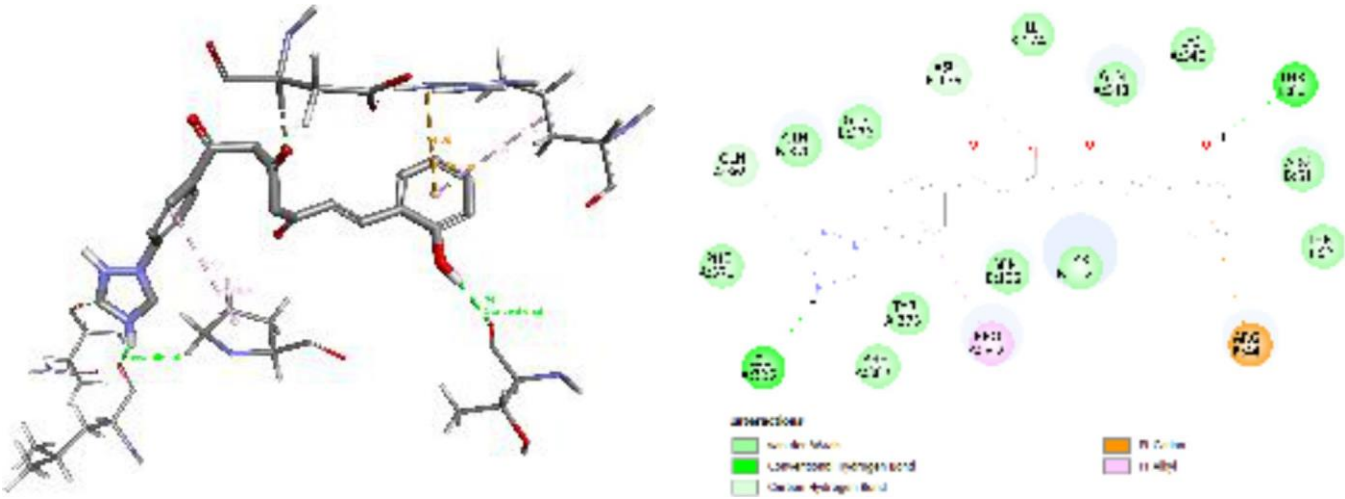


Fig. 1. Predicted binding mode and two-dimensional interaction of **AM-6** in the COX-2 active site

characteristics of **AM 1-8**. All eight analogues exhibited a predicted bioavailability score of 0.55 and high gastrointestinal absorption, with no PAINS alerts detected. The synthetic accessibility scores ranged from 2.77 to 5.09 (Table-2), which support the computational assessment of their potential for further structural optimization. The molecular structures contain α,β-unsaturated carbonyl groups that may act as Michael acceptors and a 1,3,5-triketone framework capable of metal coordination [14,15].

The toxicological profiles of compounds **AM 1-8** were estimated using the ProTox-II and all analogues were assigned toxicity class 4, with predicted oral LD_{50} values ranging from 536 to 2000 mg/kg (Table-3). The predicted probabilities varied across the toxicity endpoints, with hepatotoxicity (0.50-0.61), cardiotoxicity (0.70-0.83), carcinogenicity (0.52-0.69), mutagenicity (0.58-0.76) and cytotoxicity (0.63-0.76). Predictions for the blood-brain barrier (BBB), estrogen receptor (ER), p53, CYP3A4 and CYP2E1 endpoints ranged from 0.75-0.88, 0.77-0.86, 0.71-0.79, 0.50-0.70 and 0.93-0.99, respectively.

Anti-inflammatory activity: The *in vivo* anti-inflammatory activity of compounds **AM 1-8** was evaluated using the carrageenan-induced paw edema model. The disease-control group exhibited a progressive increase in paw volume during the

TABLE-2
SwissADME-PREDICTED DRUG-LIKENESS AND PHARMACOKINETIC PROPERTIES OF SYNTHESIZED COMPOUNDS **AM-1–AM-8**

Compound	Log-p	Muegge	Egan	Veber	Ghose	Lipinski	H-bond donors	H-bond acceptors	rotatable bonds	Bioavailability score	GI absorption	PAINS	Synthetic accessibility
AM-1		0	0	0	0	0	0	5	8	0.55	High	0	5.09
AM-2		0	0	0	0	0	0	5	8	0.55	High	0	2.77
AM-3		0	0	0	0	0	1	5	8	0.55	High	0	2.77
AM-4		0	0	0	0	0	0	5	9	0.55	High	0	2.79
AM-5		0	0	0	0	0	1	6	9	0.55	High	0	3.04
AM-6		0	0	0	0	0	1	6	8	0.55	High	0	2.85
AM-7		0	0	0	0	0	0	7	9	0.55	High	0	2.88
AM-8		0	0	0	0	0	0	7	9	0.55	High	0	3.16

TABLE-3
ProTox-II PREDICTED TOXICITY PROFILES OF SYNTHESIZED COMPOUNDS **AM-1–AM-8**

Compound	LD_{50} (mg/kg)	Toxicity class	Prediction accuracy (%)	Hepatotoxicity	Cardiotoxicity	Carcinogenicity	Mutagenicity	cytotoxicity	BBB-barrier	ER	P-53	CYP3A4	CYP2E1
AM-1	1600	4	54.26	0.53	0.80	0.55	0.66	0.75	0.87	0.86	0.77	0.66	0.95
AM-2	1600	4	54.26	0.51	0.82	0.62	0.59	0.76	0.88	0.85	0.77	0.50	0.93
AM-3	1600	4	54.26	0.54	0.80	0.57	0.68	0.74	0.88	0.84	0.73	0.54	0.98
AM-4	1600	4	54.26	0.61	0.80	0.54	0.59	0.66	0.84	0.85	0.79	0.53	0.94
AM-5	536	4	54.26	0.50	0.74	0.52	0.58	0.71	0.82	0.80	0.73	0.51	0.98
AM-6	1600	4	54.26	0.57	0.83	0.54	0.61	0.73	0.75	0.77	0.71	0.70	0.99
AM-7	1000	4	54.26	0.56	0.79	0.69	0.76	0.72	0.77	0.84	0.76	0.54	0.97
AM-8	2000	4	54.26	0.55	0.70	0.52	0.59	0.63	0.77	0.81	0.75	0.52	0.99

observation period, reaching 7.65 at 150 min. Diclofenac sodium (25 mg/kg, p.o.) reduced paw volume to 4.80 at the corresponding time point (Table-4). All the eight synthesized analogues showed lower paw-volume values than the disease control group, although the magnitude of the response varied with the aromatic substituent.

At 150 min, compound **AM-6** exhibited the lowest paw volume (4.05) among the synthesized compounds. The response of compound **AM-6** is higher than that of the other tested analogues and was accompanied by a pronounced reduction in paw volume during the later observation period. Its final paw-volume value was also lower than that recorded for diclofenac sodium. The differences between the treated and disease-control groups became more apparent at 120 and 150 min. The later phase of carrageenan-induced inflammation involves prostaglandin synthesis and other inflammatory mediators, such as kinins, nitric oxide, cytokines and reactive oxygen species [7,10,11]. The observed time-dependent reduction in paw edema is compatible with an effect on inflammatory pathways, although the specific mechanism remains unresolved.

Structure–activity relationship: The substituent-dependent biological responses were examined using paw volume at 150 min as the comparative parameter (Table-5). Compound **AM-6**, containing an *ortho*-hydroxy substituent, exhibited the lowest paw volume, whereas compound **AM-8**, bearing a 4-hydroxy-3-methoxyphenyl group, showed the highest value among the treated groups. This difference indicates that the presence of a phenolic hydroxyl group alone does not account for the observed response. The *ortho* posi-

TABLE-4
In vivo ANTI-INFLAMMATORY ACTIVITY DATA OF SYNTHESIZED ANALOGUES (**AM-1–AM-8**) IN THE CARRAGEENAN PAW EDEMA MODEL

Time (min)	Control	Disease control	Standard	**AM-1**	**AM-2**	**AM-3**	**AM-4**	**AM-5**	**AM-6**	**AM-7**	**AM-8**
0	5.10 ± 0.01	6.44 ± 0.02	5.68 ± 0.01	5.75 ± 0.01	5.65 ± 0.01	5.70 ± 0.01	5.58 ± 0.01	5.62 ± 0.01	5.50 ± 0.01	5.62 ± 0.01	6.49 ± 0.03
30	5.45 ± 0.01	6.70 ± 0.01	5.55 ± 0.01	5.62 ± 0.01	5.52 ± 0.01	5.58 ± 0.01	5.45 ± 0.01	5.48 ± 0.01	5.25 ± 0.01	5.48 ± 0.01	6.33 ± 0.04
60	6.10 ± 0.01	7.15 ± 0.01	5.35 ± 0.01	5.48 ± 0.01	5.38 ± 0.01	5.42 ± 0.01	5.28 ± 0.01	5.32 ± 0.01	4.95 ± 0.01	5.34 ± 0.01	6.13 ± 0.04
90	6.55 ± 0.01	7.40 ± 0.01	5.15 ± 0.01	5.30 ± 0.01	5.20 ± 0.01	5.25 ± 0.01	5.10 ± 0.01	5.12 ± 0.01	4.65 ± 0.01	5.14 ± 0.01	5.95 ± 0.04
120	6.80 ± 0.01	7.55 ± 0.01	4.95 ± 0.01	5.15 ± 0.01	5.05 ± 0.01	5.10 ± 0.01	4.92 ± 0.01	4.95 ± 0.01	4.35 ± 0.01	4.97 ± 0.01	5.77 ± 0.04
150	6.95 ± 0.01	7.65 ± 0.01	4.80 ± 0.01	5.00 ± 0.01	4.90 ± 0.01	4.95 ± 0.01	4.75 ± 0.01	4.78 ± 0.01	4.05 ± 0.01	4.80 ± 0.01	5.63 ± 0.04

TABLE-5
PHYSICO-CHEMICAL SUBSTITUENT DESCRIPTORS, MOLECULAR DOCKING SCORES AND PAW VOLUME OF SYNTHESIZED ANALOGUES

Compound	Ar′ substituent	σ_p	π	Docking score (kcal/mol)	Paw volume at 150 min (mm)
AM-1	4-Cl	+0.23	+0.71	–7.9	5.00
AM-2	H	0.00	0.00	–7.8	4.90
AM-3	2-Cl	*ortho*	+0.71	–7.9	4.95
AM-4	4-$N(CH_3)_2$	–0.83	+0.18	–7.1	4.75
AM-5	4-OCH_3	–0.27	–0.02	–6.4	4.78
AM-6	2-OH	*ortho*	–0.67	–8.7	4.05
AM-7	2-NO_2	*ortho*	–0.28	–7.6	4.80
AM-8	4-OH, 3-OCH_3	–0.37 (4-OH)	–0.67/–0.02	–7.7	5.63

tion of the hydroxyl group in **AM-6** may influence molecular conformation or permit intramolecular hydrogen bonding.

The *para* electron-donating substituents in compounds **AM-4** and **AM-5** were associated with lower paw volumes than the unsubstituted analogue **AM-2**. Compound **AM-7** exhibited a comparable response to **AM-4** and **AM-5**. This pattern does not support a simple relationship between electronic effects and anti-inflammatory activity. The chloro substituted compounds **AM-1** and **AM-3** showed less pronounced reductions in paw volume than **AM-6**. Moreover, the activity difference between **AM-6** and **AM-8** may involve positional and conformational effects of the hydroxyl group, thus, the present series identifies the *ortho*-hydroxy analogue **AM-6** as the most active compound under the experimental conditions employed.

The numerical differences among **AM-1**, **AM-2**, **AM-3**, **AM-4**, **AM-5 and AM-7** are relatively small, with paw-volume differences of approximately 0.10-0.25 units at 150 min. Their relative ranking should not be considered statistically established without appropriate statistical analysis. The reported Spearman correlation between docking score and *in vivo* activity (ρ = -0.16) indicates a weak relationship between the two parameters. **AM-5**, despite having the least favourable docking score, exhibited one of the better paw-volume responses, whereas **AM-8** showed a comparatively weak biological response despite its intermediate docking score.

Conclusion

The present study describes the synthesis and biological evaluation of eight 1,2,4-triazole-based hept-6-ene-1,3,5-trione analogues (**AM 1-8**). The synthesized compounds were obtained in moderate to good yields and characterized using spectroscopic techniques. The carrageenan-induced paw edema model revealed reductions in paw volume across the tested series, with compound **AM-6** bearing an *ortho*-hydroxyphenyl substituent exhibiting the most pronounced response at 150 min. The differences observed between compounds **AM-6** and **AM-8** suggest that the position of the hydroxyl group may influence the biological response and provide a useful direction for further structural modification. Molecular docking identified compound **AM-6** as the analogue with the most favourable predicted COX-2 binding score. Swiss-ADME and ProTox-II analyses provided preliminary information on drug-likeness and potential toxicological liabilities, which remain to be confirmed experimentally. The present findings identify **AM-6** as a promising lead structure for further investigation of this triazole-triketone series.

ACKNOWLEDGEMENTS

The authors gratefully acknowledge the Principal, Dr. K. Mangathyaru, Pravara Rural College of Pharmacy, for providing excellent research facilities. Sincere appreciation is extended to Sciquaint Innovations Private Limited, Pune, India, for technical assistance throughout the research work.

CONFLICT OF INTEREST

The authors declare that there is no conflicts of interest regarding the publication of this article.

DECLARATION OF AI-ASSISTED TECHNOLOGIES

During the preparation of this manuscript, the authors used an AI-assisted tool(s) to improve the language and no data, results or scientific conclusions were generated by AI. All analyses, interpretations and conclusions are the authors' own. The authors reviewed and edited the content and take full responsibility for the published work.

REFERENCES

1. N.K. Sahu, S.S. Balbhadra, J. Choudhary and D.V. Kohli, *Curr. Med. Chem.*, **19**, 209 (2012); https://doi.org/10.2174/092986712803414132
2. C. Zhuang, W. Zhang, C. Sheng, W. Zhang, C. Xing and Z. Miao, *Chem. Rev.*, **117**, 7762 (2017); https://doi.org/10.1021/acs.chemrev.7b00020
3. R. Kharb, P.C. Sharma and M.S. Yar, *J. Enzyme Inhib. Med. Chem.*, **26**, 1 (2011); https://doi.org/10.3109/14756360903524304
4. B. Khan, A. Naiyer, F. Athar, S. Ali and S.C. Thakur, *J. Biomol. Struct. Dyn.*, **39**, 457 (2021); https://doi.org/10.1080/07391102.2019.1711193
5. A. Ayati, S. Emami and A. Foroumadi, *Eur. J. Med. Chem.*, **109**, 380 (2016); https://doi.org/10.1016/j.ejmech.2016.01.009
6. K. Bozorov, J. Zhao and H.A. Aisa, *Bioorg. Med. Chem.*, **27**, 3511 (2019); https://doi.org/10.1016/j.bmc.2019.07.005
7. B.B. Aggarwal, C. Sundaram, N. Malani and H. Ichikawa, *Adv. Exp. Med. Biol.*, **595**, 1 (2007); https://doi.org/10.1007/978-0-387-46401-5_1
8. G.S. Firestein, *Nature*, **423**, 356 (2003); https://doi.org/10.1038/nature01661
9. J.R. Vane, *Nat. New Biol.*, **231**, 232 (1971); https://doi.org/10.1038/newbio231232a0
10. G.A. Fitzgerald and C. Patrono, *N. Engl. J. Med.*, **345**, 433 (2001); https://doi.org/10.1056/NEJM200108093450607
11. R. Botting, *J. Physiol. Pharmacol.*, **57(S5)**, 113 (2006).
12. K.C. Duggan, D.J. Hermanson, J. Musee, J.J. Prusakiewicz, J.L. Scheib, B.F. Carter, S. Banerjee, J.A. Oates and L.J. Marnett, *J. Biol. Chem.*, **285**, 34950 (2010); https://doi.org/10.1074/jbc.M110.162982
13. J.L. Wang, D. Limburg, M.J. Graneto, J. Springer, J.R. Hamper, S. Liao, J.L. Pawlitz, R.G. Kurumbail, T. Maziasz, J.J. Talley, J.R. Kiefer and J. Carter, *Bioorg. Med. Chem. Lett.*, **20**, 7159 (2010); https://doi.org/10.1016/j.bmcl.2010.07.054
14. A. Daina, O. Michielin and V. Zoete, *Sci. Rep.*, **7**, 42717 (2017); https://doi.org/10.1038/srep42717
15. P. Banerjee, A.O. Eckert, A.K. Schrey and R. Preissner, *Nucleic Acids Res.*, **46**, W257 (2018); https://doi.org/10.1093/nar/gky318
16. C.A. Winter, E.A. Risley and G.W. Nuss, *Proc. Soc. Exp. Biol. Med.*, **111**, 544 (1962); https://doi.org/10.3181/00379727-111-27849
17. O. Trott and A.J. Olson, *J. Comput. Chem.*, **31**, 455 (2010); https://doi.org/10.1002/jcc.21334
18. G.M. Morris, R. Huey, W. Lindstrom, M.F. Sanner, R.K. Belew, D.S. Goodsell and A.J. Olson, *J. Comput. Chem.*, **30**, 2785 (2009); https://doi.org/10.1002/jcc.21256
19. C.A. Lipinski, F. Lombardo, B.W. Dominy and P.J. Feeney, *Adv. Drug Deliv. Rev.*, **46**, 3 (2001); https://doi.org/10.1016/S0169-409X(00)00129-0
20. D.F. Veber, S.R. Johnson, H.Y. Cheng, B.R. Smith, K.W. Ward and K.D. Kopple, *J. Med. Chem.*, **45**, 2615 (2002); https://doi.org/10.1021/jm020017n
21. A.K. Ghose, V.N. Viswanadhan and J.J. Wendoloski, *J. Comb. Chem.*, **1**, 55 (1999); https://doi.org/10.1021/cc9800071
22. W.J. Egan, K.M. Merz Jr. and J.J. Baldwin, *J. Med. Chem.*, **43**, 3867 (2000); https://doi.org/10.1021/jm000292e
23. P. Ertl and A. Schuffenhauer, *J. Cheminform.*, **1**, 8 (2009); https://doi.org/10.1186/1758-2946-1-8